From Fossil Resources to Renewable Resources: Synthesis, Structure, Properties and Comparison of Terephthalic Acid-2,5-Furandicarboxylic Acid-Diol Copolyesters

Jiang Min, Lu Tingting, Zhang Qiang, Chen Ying and Zhou Guangyuan*

Key Laboratory of Polymer Ecomaterials, Changchun Institute of Applied Chemistry, Chinese Academy of Sciences, No. 5625, Ren Min Street, Changchun, 130022, Jilin, China

Received December 3, 2014; Accepted February 28, 2015

ABSTRACT: Novel copolyesters were successfully synthesized from terephthalic acid (TPA), 2,5-furandicarboxylic acid (FDCA) and ethylene glycol, 1,3-propanediol, 1,4-butanediol, 1,6-hexanediol and 1,8-octanediol via direct esterification method by using tetrabutyl titanate (TBT) as catalyst. The copolyesters were characterized by nuclear magnetic resonance spectroscopy (^{1}H-NMR), gel permeation chromatography (GPC), X-ray diffraction (XRD), differential scanning calorimetry (DSC), thermogravimetric analysis (TGA) and tensile tests. The results of GPC showed that all of the copolyesters had high molecular weight, with an average molecular weight (Mw) more than 1×10^4 g/mol. The results of ^{1}H-NMR showed that the copolyesters were random copolymers which compositions were well controlled by the feed ratio of the diacid monomers, and the degrees of randomness (B) values were near to 1.0 and 1.40. The results of DSC showed that all of the copolyesters had one glass transition temperature (T_g) and the T_gs were between those of corresponding homopolyesters. The results of TGA showed that the copolyesters were thermally stable up to 370°C and had similar thermal stabilities to corresponding homopolyesters. The results of tensile tests showed that some of the PETF and PTTF copolyesters had better tensile strength and tensile modules, and PBTF, PHTF and POTF copolyesters had higher elongation at break.

KEYWORDS: Renewable resource, 2,5-furandicarboxylic acid, copolyester, direct esterification method, structure and properties

1 INTRODUCTION

Polymeric materials from readily renewable resources, or biobased polymers, have already gained an established position among synthetic materials in both academic and industrial fields. Renewable polymers are being developed to replace petrochemical products in a wide array of applications [1–3]. People have begun to take an interest in finding new biobased polymers and monomers. Biobased monomers have been proved to be very well-suited alternatives for fossil fuel-based monomers. The facts show that polymers based on these monomers have many advantages in many fields [4–7].

Furan-based molecules are a particularly attractive class of biobased monomers. Within this class there is a monomer named 2,5-furandicarboxylic acid (FDCA). It is a member of the furan family and can be formed from C6 sugars and polysaccharides based on C5 glycosidic units [8–10]. Honeys, fruits, vegetables, and so on, are rich in those compositions. Furthermore, FDCA has two carboxyl groups and its structure is similar to terephthalic acid (TPA); it has been considered as a replacement for TPA [11–13]. Moreover, FDCA was indentified by the US Department of Energy as one of 12 priority chemicals likely to play an important role in establishing the chemistry industry [14]. Importantly, FDCA has great potential as a monomer to synthesize polyester, polyurethane [15,16] and polyamide [17,18]. Especially in recent years, polyesters based on FDCA have gained more attention. And researchers have conducted lots of work on them, including homopolyesters [19–28,38–41] and copolyesters [31–34,42,43], mostly with the aim of developing new polymer materials and alternatives in engineering plastic such as PET and PBT. In 2012, Wu *et al.* [31] reported that copolyesters poly(butylene succinate-butylene furandicarboxylate) were synthesized

---

**Corresponding author*: gyzhou@ciac.ac.cn

DOI: 10.7569/JRM.2014.634139

from FDCA, succinic acid and 1,4-butanediol via esterification and polycondensation by using tetrabutyl titanate (TBT) and TBT/La(acac)_3 as catalysts. In 2012, Ma *et al.* [32] displayed furan-based copolyesters which were synthesized via polytransesterification of FDCA, ethylene glycol and 1,4-butylene glycol using TBT as catalyst. In 2013, Yu *et al.* [33] showed that copolymers poly(ethylene 2, 5-furancarboxylate-co-ethylene succinate) were prepared based on FDCA, succinic acid and ethylene glycol by using tetrabutyl titanate as catalysts. In 2013, Sousa *et al.* [34] displayed new copolymers done by random copolymerization of bis(2-hydroxyethyl) terephthalate and bis(hydroxyethyl)-2,5-furandicarboxylate in which antimony(III) oxide was used as catalyst. We always wondered whether FDCA could partly replace TPA to synthesize copolyesters. Recently, we tried to prepare PETF copolyesters from FDCA, TPA and ethylene glycol via direct esterificaiton method [42,43], which gave us some hope. The results showed that FDCA could partly replace TPA to synthesize PETF copolyesters. The PETF copolyesters had one single value of glass-transition temperature (T_g) and their thermal stability was similar to that of PEF and PET. Some of the PETF copolyesters had better mechanical properties than that of PET, for example, PETF-10 (FDCA: TPA=1:9mol/mol), as shown in Table 5.

As is known to all, the manufacture of FDCA would likely be from hydroxymethylfurfural (HMF); an important intermediate for many furan-based monomers. Although FDCA based on an improved route to HMF synthesis [35–37] is being intensely pursued by academics and industrial scientists, its degree of commercialization and price do not have any advantages to that of TPA. So, we wondered whether a series of copolyesters could be prepared from FDCA, TPA and different diols.

Thus, this article describes the synthesis, structure, thermal and mechanical properties of five copolyester series prepared from FDCA, TPA and ethylene glycol [41,42], 1,3-propanediol, 1,4-butanediol, 1,6-hexanediol and 1,8-octanediol via direct esterification method. Tetrabutyl titanate (TBT) was used as catalyst. The copolyesters were characterized by ^{1}H-NMR, GPC, XRD, DSC, TGA and tensile testing. To access the potential of partly replacing FDCA with TPA, the properties of copolyesters and comparisons of the structure, thermal and mechanical properties of copolyesters with corresponding homopolyesters were conducted.

2 EXPERIMENTAL

2.1 Materials

2,5-Furandicarboxylic acid (FDCA, pure grade >99.5%) was obtained from Satachem Co., Ltd.; terephthalic acid (TPA) was purchased from J&K Chemical Ltd.; 1, m^2 3-propanediol, 1,4-butanediol, 1,6-hexanediol and 1,8-octanediol were purchased from China National Medicines Corporation Ltd.; 1,1,2,2-tetrachloroethane and phenol were purchased from Beijing Chemical Works; and tetrabutyl titanate (TBT, 99%) was purchased from Tianjin No.1 Chemical Reagent Factory.

2.2 Characterization

2.2.1 *Nuclear magnetic resonance spectroscopy (^{1}H-NMR)*

The ^{1}H-NMR measurement was carried out on a Varian Mercury Plus 400 MHz and 600 MHz ^{1}H-NMR spectrometer which was operated at room temperature. The purified copolyester samples were dissolved in CF_3COOD with tetramethylsilane (TMS) as the internal reference.

2.2.2 *Molecular weights and distribution*

Weight-average molecular weight (Mw), number-average molecular weight (Mn) and their polydispersity index (PDI) were obtained by gel permeation chromatography using a liner DMF column and a Waters 1515 HPLC with OPTILAB DSP interferometric refractometer (Wyatt Technology) as detector. The eluent was hexafluoroisopropanol at a flow rate of 1.0 ml/min at 40°C. Monodispersed polymethyl methacrylate standard (molecular weight, 6000 to 1000000 g/mol) was used.

2.2.3 *Specific viscosity measurement*

The specific viscosities (η_{sp}) of samples were measured at a concentration of 0.5 g/dL in 1,1,2,2-tetrachloroethane/phenol (1:1 w/w) under 25°C by using an Ubbelohde viscometer by the standard method.

η_{sp}/C expressed reduced viscosity and its unit was dL/g. C was the concentration of 0.5 g/dL furan-aromatic polyesters in 1,1,2,2-tetrachloroethane/phenol (1:1 w/w) under 25°C.

2.2.4 *X-ray diffraction tests*

The X-ray diffraction (XRD) patterns of samples were carried out on a PW1700s X-ray diffractometer, using Cu Kα radiation.

2.2.5 *DSC characterization*

The DSC analyses were performed with a Mettler Toledo DSC 1 differential scanning calorimeter (DSC), calibrated with zinc standards. Samples of 6 ± 0.1 mg were used in the test. The samples were sealed in aluminum pans and heated to 270°C at a heating rate of 5°C/min in nitrogen.

2.2.6 *TGA characterization*

The thermal stability was determined by thermogravimetric analysis (TGA) using Mettler Toledo TGA/DSC 1 series apparatus. The thermal analyzer was temperature calibrated by using the Curie point of nickel as a reference. Samples (6±0.5 mg) were heated from 30°C to 600°C at a heating rate of 10°C/min in nitrogen and air.

2.2.7 *Tensile tests*

The tensile tests were performed using an Instron-1121 tester with a strain rate of 2 mm/min at room temperature. Three dumbbell-shaped specimens (15×3.23×3.20 mm) were employed in each testing to determine average of tensile modulus (E), tensile strength (σ_m) and elongation at break (ε_b).

2.3 Polymerization Procedure

Copolyesters and homopolyesters were synthesized via solvent-free direct esterification method and tetrabutyl titanate (TBT) was used as catalyst. A mixture of TPA, FDCA, diols and TBT (0.3‰mol/mol diacid) were reacted in a 50 ml three-neck round-bottom flask. The diols were comprised of ethylene glycol, 1,3-propanediol, 1,4-butanediol, 1,6-hexanediol and 1,8-octanediol. The stoichiometric ratio between FDCA with ethylene glycol, 1,3-propanediol or 1,4-butanediol was 1:1.6. The stoichiometric ratio between FDCA with 1,6-hexanediol or 1,8-octanediol was 1:1.2. Before reaction, the three-neck, round-bottom flask was replaced by nitrogen at least three times to remove air. For the first step, the reaction was carried out at 230–270°C protected by nitrogen. For the second step, the pressure in the reactor was decreased gradually to 70 Pa and the polycondension was carried out at 240–270°C. The final polymers were purified by being dissolved in *o*-chlorophenol and being precipitated in methanol three times, and then being dried in a vacuum oven at 120°C for 72 h (for the use of NMR and GPC testing).

Table 1 lists the synthesis conditions and η_{sp}/C of copolyesters and homopolyesters in detail.

PEF: poly (ethylene 2, 5-furandicarboxylate)
PTF: poly (trimethylene 2, 5-furandicarboxylate)
PBF: poly (butylene 2, 5-furandicarboxylate)
PHF: poly (hexylene 2, 5-furandicarboxylate)
POF: poly (octylene 2, 5-furandicarboxylate)
PEF, PTF, PBF, PHF and POF were called FDCA-based homopolyesters.

PET: poly (ethylene terephthalate)
PTT: poly (trimethylene terephthalate)
PBT:poly(butylene terephthalate)
PHT: poly (hexylene terephthalate)
POT: poly (octylene terephthalate)
PET, PTT, PBT, PHT and POT were called TPA-based homopolyesters.
PETF: poly (ethylene terephthalate-co-ethylene 2, 5-furandicarboxylate)
PTTF: poly (trimethylene terephthalate-co- trimethylene 2, 5-furandicarboxylate)
PBTF: poly (butylene terephthalate-co-butylene 2, 5-furandicarboxylate)
PHTF: poly (hexylene terephthalate-co-hexylene 2, 5-furandicarboxylate)
POTF: poly (octylene terephthalate-co-octylene 2, 5-furandicarboxylate)

PETF-50: 1H-NMR (Figure 3, CF3COOD, δ/ppm): 8.07 (s, 4H, H2 H3 H5 H6 benzene ring); 7.27, (s 2H, H3 H4 furan ring); 4.76 (t, 4H, benzene ring-C$\underline{H}_2$-C$\underline{H}_2$-benzene ring), 4.74 (t, 2H, benzene ring -C$\underline{H}_2$-CH$_2$-furan ring), 4.72 (t, 2H, benzene ring-CH$_2$-C$\underline{H}_2$-furan ring), 4.69 (t, 4H, furan ring-C$\underline{H}_2$-C$\underline{H}_2$-furan ring) [42].

PTTF-50: ^{1}H-NMR (Figure 3, CF$_3$COOD, δ/ppm): 7.93 (s, 4H, H2 H3 H5 H6 benzene ring); 7.13, (s 2H, H3 H4 furan ring); 4.45, (t 4H, benzene ring-C$\underline{H}_2$-CH$_2$-C$\underline{H}_2$-benzene ring); 4.44, (t 2H, benzene ring-C$\underline{H}_2$-CH$_2$-CH$_2$-furan ring); 4.42, (t 2H, benzene ring-CH$_2$-CH$_2$-C$\underline{H}_2$-furan ring); 4.41, (t 4H, furan ring-C$\underline{H}_2$-CH$_2$-C$\underline{H}_2$-furan ring); 2.16, (q 2H, -CH$_2$-C$\underline{H}_2$-CH$_2$-).

PBTF-50: ^{1}H-NMR (Figure 3, CF$_3$COOD, δ/ppm): 8.40 (s, 4H, H2 H3 H5 H6 benzene ring); 7.58, (s 2H, H3 H4 furan ring); 4.80, (t 4H, benzene ring-C$\underline{H}_2$-CH$_2$-CH$_2$-C$\underline{H}_2$-benzene ring); 4.79, (t 2H, benzene ring-C$\underline{H}_2$-CH$_2$-CH$_2$-CH$_2$-furan ring); 4.78, (t 2H, furan ring-C$\underline{H}_2$-CH$_2$-CH$_2$-CH$_2$-benzene ring); 4.77, (t 4H, furan ring-C$\underline{H}_2$-CH$_2$-CH$_2$-C$\underline{H}_2$-furan ring); 2.23-2.24, (q 4H, -CH$_2$-C$\underline{H}_2$-C$\underline{H}_2$-CH$_2$-)

PHTF-50: ^{1}H-NMR (Figure 3, CF$_3$COOD, δ/ppm): 8.36 (s, 4H, H2 H3 H5 H6 benzene ring); 7.54, (s 2H, H3 H4 furan ring); 4.70, (t 4H, benzene ring-C$\underline{H}_{2-}$CH$_2$-CH$_{2-}$CH$_{2-}$CH$_2$-C$\underline{H}_2$-benzene ring); 4.69, (t 2H, benzene ring-C$\underline{H}_{2-}$CH$_2$-CH$_{2-}$CH$_{2-}$CH$_2$-CH$_2$-furan ring); 4.68, (t 2H, furan ring-C$\underline{H}_{2-}$CH$_2$-CH$_{2-}$CH$_{2-}$CH$_2$-CH$_2$-benzene ring); 4.67, (t 4H, furan ring-C$\underline{H}_{2-}$CH$_2$-CH$_{2-}$CH$_{2-}$CH$_2$-C$\underline{H}_2$-furan ring); 2.13-2.08, (m 4H, -CH$_{2-}$C$\underline{H}_2$-CH$_{2-}$CH$_{2-}$C$\underline{H}_2$-CH$_2$-); 1.82-1.76, (m 4H, -CH$_{2-}$CH$_2$-C$\underline{H}_{2-}$C$\underline{H}_{2-}$CH$_2$-CH$_2$-).

POTF-50: ^{1}H-NMR (Figure 3, CF$_3$COOD, δ/ppm): 8.36 (s, 4H, H2 H3 H5 H6 benzene ring); 7.53, (s 2H, H3 H4 furan ring), 4.68, (t 4H, benzene ring-C$\underline{H}_2$-CH$_2$-CH$_2$-CH$_2$-CH$_2$-CH$_2$-CH$_2$-C$\underline{H}_2$-benzene

Table 1 The synthesis conditions and η_{sp}/C of copolyesters and homopolyesters

Sample	Etep(°C)	Tp(min)	Ptep(°C)	Pt(min)	η_{sp}/C(dL/g)	Sample	Etep(°C)	Tp(min)	Ptep(°C)	Pt(min)	η_{sp}/C(dL/g)
PET[41]	245	425	270	240	0.80	PHT	260	360	265	400	1.08
PETF-10[41]	260	385	270	120	1.16	PHTF-10	255	340	260	300	1.18
PETF-30[41]	245	215	255	180	0.95	PHTF-30	250	320	260	300	1.19
PETF-50[41]	240	133	255	180	0.96	PHTF-50	250	300	260	240	1.01
PETF-70[41]	240	136	250	180	0.97	PHTF-70	250	215	250	240	1.25
PETF-90[41]	240	100	250	300	1.03	PHTF-90	240	140	245	240	1.24
PEF[41]	230	85	250	240	0.85	PHF	235	68	240	300	1.27
PTT	255	170	270	120	1.03	POT	265	365	265	300	1.52
PTTF-10	260	150	270	180	0.91	POTF-10	265	340	265	300	1.01
PTTF-30	260	115	270	180	0.82	POTF-30	260	330	265	330	1.07
PTTF-50	260	90	270	180	0.85	POTF-50	260	315	265	320	1.30
PTTF-70	260	95	270	180	0.86	POTF-70	260	280	265	300	1.25
PTTF-90	240	90	260	180	0.88	POTF-90	260	210	265	240	1.87
PTF	230	50	240	240	0.99	POF	240	60	260	180	1.33
PBT	250	310	270	120	1.72						
PBTF-10	250	265	270	225	1.21						
PBTF-30	250	265	255	240	1.14						
PBTF-50	240	200	255	240	1.04						
PBTF-70	240	150	255	240	0.83						
PBTF-90	240	90	255	240	0.83						
PBF	230	110	245	120	1.17						

E_{tep}: Esterification temperature; T_p: Time of arriving at clear point P_{tep}: Polycondensation temperature; P_t: Polycondensation time ring); 4.68, (t 4H, benzene ring-$C\underline{H}_2$-CH_2-CH_2-CH_2-CH_2-CH_2-CH_2-$C\underline{H}_2$-benzene ring); 4.67, (t 2H, benzene ring-$C\underline{H}_2$-CH_2-CH_2-CH_2-CH_2-CH_2-CH_2-furan ring); 4.66, (t 2H, furan ring-$C\underline{H}_2$-CH_2-CH_2-CH_2-CH_2-CH_2-CH_2-CH_2-benzene ring); 4.65, (t 4H, furan ring-$C\underline{H}_2$-CH_2-CH_2-CH_2-CH_2-CH_2-CH_2-$C\underline{H}_2$-furan ring); 2.09-2.03 (m 4H, -CH_2-$C\underline{H}_2$-CH_2-CH_2-CH_2-CH_2-$C\underline{H}_2$-CH_{2-}); 1.73-1.64, (m 8H, -CH_2-CH_2-$C\underline{H}_2$-$C\underline{H}_2$-$C\underline{H}_2$-$C\underline{H}_2$-CH_2-$CH_{2-)}$.

3 RESULTS AND DISCUSSION

Copolyesters based on TPA, FDCA and different diols in full composition range were synthesized via one-step direct esterification method, shown in Scheme 1. TBT was used as catalyst.

Table 1 displayed the optimized synthesis conditions and η_{sp}/C of all copolyesters and corresponding homopolyesters. Table 2 showed the theoretical and real mole ratios of TPA and FDCA, and the randomness B of copolyesters. TBT (0.3‰mol/mol diacid) was used as catalyst for the whole esterification and polycondensation process. For PETF, PTTF and PBTF copolyesters, molar ratio of diacid to diol was 1:1.6. For PHTF and POTF copolyesters, molar ratio of diacid to diol was 1:1.2. Obviously, the consumptions of ethylene glycol, 1,3-propanediol and 1,4-butanediol were more than that of 1,6-hexanediol and 1,8-octanediol. It was believed that the lower consumptions of 1,6-hexanediol and 1,8-octanediol [41] were mainly caused because they had lower volatility at esterification temperature and they were diffcult to draw out at the polycondensation stage. The high consumptions of ethylene glycol [39], 1,3-propanediol and 1,4-butanediol were basically due to their higher volatility at esterificaiton temperature. The direct esterification method was selected because this method is usually characterized as an easy, convenient and low byproduct method in the polyester industry. Actually, the results showed that the direct esterification method could be used very well not only for homopolyesters [38–40], but also for copolyesters. Copolyesters with η_{sp}/C ranging from 0.80 to 1.30 dL/g could be prepared by adjusting esterification temperature, esterification time, polycondensation temperature and polycondensation time, with synthesis conditions that were obviously different from that of homopolyesters (Table 1). From Table 1, it can also be seen that the esterification temperature of some copolyesters and FDCA-based homopolyesters were similar to or in some cases lower than that of TPA-based polyesters. Esterification time decreased with increasing FDCA content. For example, the esterification temperatures and time of PETF-70, PETF-90 and PEF were obviously lower than that of PET. It was possible that the esterification product or oligomer of FDCA was easy to dissolve in melted diol and oligomer. In that case, the rate of esterification reaction was promoted; esterification reaction did not need too high temperature and too much time. Furthermore, Table 2 indicates that the real mole ratios of TPA and FDCA in copolyesters were similar to theoretical mole ratios, which proves the reaction activity of FDCA and TPA was similar.

Table 3 illustrates the molecular characteristics of copolyesters. It can be seen that all copolyesters had high molecular weight with the weight-average molecular weight ranging from 3.48×10^4 to 42.56×10^4 g/mol. The polydispersity index (PDI) of all copolyesters ranged from 1.40 to 3.01. In comparison to TPA-based polyesters, such as PET, PTT, PBT, PHT and POT, which were a white to slightly yellowish solid, the synthesized copolyesters were colored product and appeared in different degrees of brown. The coloration of copolyesters was also found to depend on composition, and color darkness gradually increased with increasing FDCA content in copolyesters. Two factors could be associated with the coloration of

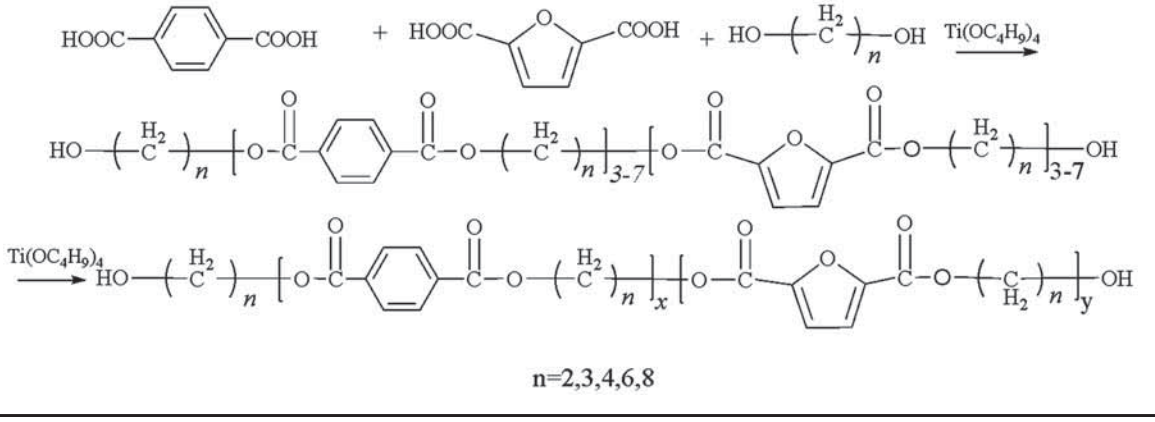

Scheme 1 The synthesis route of copolyester via direct esterification method.

Table 2 The theoretical and real mole ratios of PTA and FDCA and B of copolyesters

Sample	TPA:FDCA (molar ratio)	^{1}H-NMR (TPA:FDCA)	B	Sample	TPA:FDCA (molar ratio)	^{1}H-NMR (TPA:FDCA)	B
PET[42]	1.0:0	–	–	PHT	1.0:0	–	–
PETF-10[42]	0.9:0.1	0.83:0.10	1.02	PHTF-10	0.9:0.1	0.89:0.10	1.40
PETF-30[42]	0.7:0.3	0.68:0.30	1.02	PHTF-30	0.7:0.3	0.70:0.3	1.47
PETF-50[42]	0.5:0.5	0.50:0.50	1.01	PHTF-50	0.5:0.5	0.50:0.50	1.36
PETF-70[42]	0.3:0.7	0.32:0.70	0.98	PHTF-70HTF-900	0.3:0.7	0.30:0.70	1.46
PETF-90[42]	0.1:0.9	0.13:0.90		PHTF-90	0.1:0.9	0.10:0.90	1.42
PEF[42]	0:1.0	–	–	PHF	0:1.0	–	–
PTT	1.0:0	–	–	POT	1.0:0	–	–
PTTF-10	0.9:0.1	0.88:0.10	1.11	POTF-10	0.9:0.1	0.92:0.10	1.39
PTTF-30	0.7:0.3	0.71:0.30	1.15	POTF-30	0.7:0.3	0.70:0.30	1.41
PTTF-50	0.5:0.5	0.50:0.50	0.99	POTF-50	0.5:0.5	0.50:0.50	1.37
PTTF-70	0.3:0.7	0.30:0.70	1.03	POTF-70	0.3:0.7	0.32:0.70	1.365
PTTF-90	0.1:0.9	0.10:0.90	1.19	POTF-90	0.1:0.9	0.11:0.90	1.41
PTF	0:1.0	–	–	POF	0:1.0	–	–
PBT	1.0:0	–	–				
PBTF-10	0.9:0.1	0.87:0.10	1.04				
PBTF-30	0.7:0.3	0.70:0.30	1.02				
PBTF-50	0.5:0.5	0.52:0.50 .5	1.00				
PBTF-70	0.3:0.7	0.32:0.70	1.01				
PBTF-90	0.1:0.9	0.10:0.90	1.07				
PBF	0:1.0	–	–				

B is the degree of randomness

copolyesters. The catalyst, TBT, might lead to the coloration, as it is well-known that the use of TBT often results in the yellowing of common polyesters [44]. The second factor is was the decarboxylation of FDCA. According to de Jong *et al.* [29] and Drewitt *et al.* [30], the coloration was due to decarboxylation of FDCA under the reaction conditions. Additionally, in the experiment, it was found that the purified copolyesters were white, which shows that the color of copolyesters was mainly caused by the above two factors.

The copolyesters were also characterized by ^{1}H-NMR. The spectra were found to be consistent with the expected structures in terms of both chemical shifts and relative integrations. The ^{1}H-NMR spectra of PETF-50, PTTF-50, PBTF-50, PHTF-50 and POTF-50 were displayed in Figure 3, along with the corresponding assignments and relative integrations. The signals at about 8.00 ppm and 7.00 ppm respectively represent the methane protons of the benzene ring and furan ring for all of the copolyesters compared with the FDCA-based and TPA-based homopolyesters. For PETF-50, those four signals at 4.69–4.76 ppm represent the two methylene protons of EG in PEF and PET units. For PTTF-50, those four signals at 4.41–4.45 ppm represent the two end methylene protons of 1,3-propanediol in PTF and PTT units. The signal at 2.16 ppm represents the middle methylene proton of 1,3-propanediol in PTF and PTT units. For PBTF-50, those four signals at

Table 3 The M_n, M_w and PDI of copolyesters

Sample	$M_n(\times10^4)$	$M_w(\times10^4)$	PDI	Sample	$M_n(\times10^4)$	$M_w(\times10^4)$	PDI
PET	3.02	4.52[41]	1.50	PHT	2.48	3.48	1.40
PETF-10	1.25	1.57[41]	1.26	PHTF-10	3.58	5.53	1.55
PETF-30	7.66	22.73[41]	2.97	PHTF-30	5.46	11.94	2.18
PETF-50	12.37	36.29[41]	2.93	PHTF-50	7.17	16.98	2.37
PETF-70	19.35	48.84[41]	2.52	PHTF-70	13.04	31.61	2.42
PETF-90	3.96	12.57[41]	2.70	PHTF-90	23.26	42.56	1.83
PEF	23.98	43.14[41]	1.80	PHF	9.80	27.26	2.78
PTT	2.61	3.80	1.46	POT	3.09	4.61	1.49
PTTF-10	2.54	3.71	1.46	POTF-10	2.82	4.25	1.50
PTTF-30	4.49	9.52	2.12	POTF-30	4.76	9.38	1.97
PTTF-50	7.54	20.18	2.68	POTF-50	8.09	21.33	2.64
PTTF-70	14.64	35.22	2.41	POTF-70	9.72	29.54	3.04
PTTF-90	13.98	34.28	2.45	POTF-90	20.23	40.14	1.98
PTF	23.09	56.08	2.43	POF	13.62	29.18	2.14
PBT	3.13	4.85	1.55				
PBTF-10	3.45	5.42	1.57				
PBTF-30	4.23	8.12	1.92				
PBTF-50	6.47	15.65	2.42				
PBTF-70	6.40	18.43	2.88				
PBTF-90	9.62	28.99	3.01				
PBF	14.44	44.04	3.05				

4.77–4.80 ppm represent the two end methylene protons of 1,4-butanediol in PBF and PBT units. The signal at 2.24–2.32 ppm represents the two middle methylene protons of 1,4-butanediol. For PHTF-50, those four signals at 4.67–4.70 ppm represent the two end methylene protons of 1,6-hexanediol in PHF and PHT units. The signal at 2.08–2.13 ppm represents the two middle methylene protons next to the OCH_2. The signal at 1.76–1.82 ppm represents the two middle methylene protons at a distance from the OCH_2. For POTF-50, those four signals at 4.65–4.68 ppm represent the two end methylene protons of 1,8-octanediol in POF and POT units. The signal at 2.03–2.09 ppm represents the two middle methylene protons next to the OCH_2 of 1,8-octanediol. The signal at 1.64–1.73 ppm represents the four middle methylene protons at a distance from the OCH_2 of 1,8-octanediol. In these copolyesters, the hydrogen proton on the end methylene of diols lies in three different chemical environments, which makes hydrogen proton form four different chemical shifts in NMR. So, it also proved that the copolyesters were successfully prepared based on the obvious four signals of two end ethylene protons of diols in ^{1}H-NMR of copolyesters. The results of relative integration ratios for each methylene proton in copolyesters corresponded to those of the expected structures. As the content of the furan units increased, the relative intensity of the methylene protons of the furan ring also increased, whereas that of methylene proton of diols close to the furan ring increased gradually, as shown in P1–P5 and Table S1. The influence of the mole ratios of TPA and FDCA in the initial reaction mixture on the structure of polymer chains in different copolyesters by ^{1}H-NMR was listed in Table S1. All of the copolyesters were random copolymers, with randomness B values of PETF, PTTF and PBTF copolyesters of about 1.0, and PHTF and POTF copolyesters of about 1.40. The B values of PHTF and POTF copolyesters were more than 1 (about 1.40), which meant that some of the copolyesters were close to being alternate copolymers, and the activities of FDCA and TPA were more similar in these two reaction systems caused by long chain diol. In a word, the reactive activities of TPA and FDCA to diols were similar in these nucleophilic substitution reactions, especially when TPA and FDCA reacted with long chain diols (1,6-hexanediol and 1,8-octanediol). When TPA/FDCA molar ratio was 0.5:0.5 for PETF, PTTF, PBTF, PHTF and POTF copolyesters, the B values were closest to 1, which showed that the content of asymmetric structures in copolyesters was the most (Tables 2 and S1). It can also be seen that the contents of asymmetric structures in PETF-50, PTTF-50, PBTF-50, PHTF-50 and POTF-50 were the most in each copolyester series, as observed

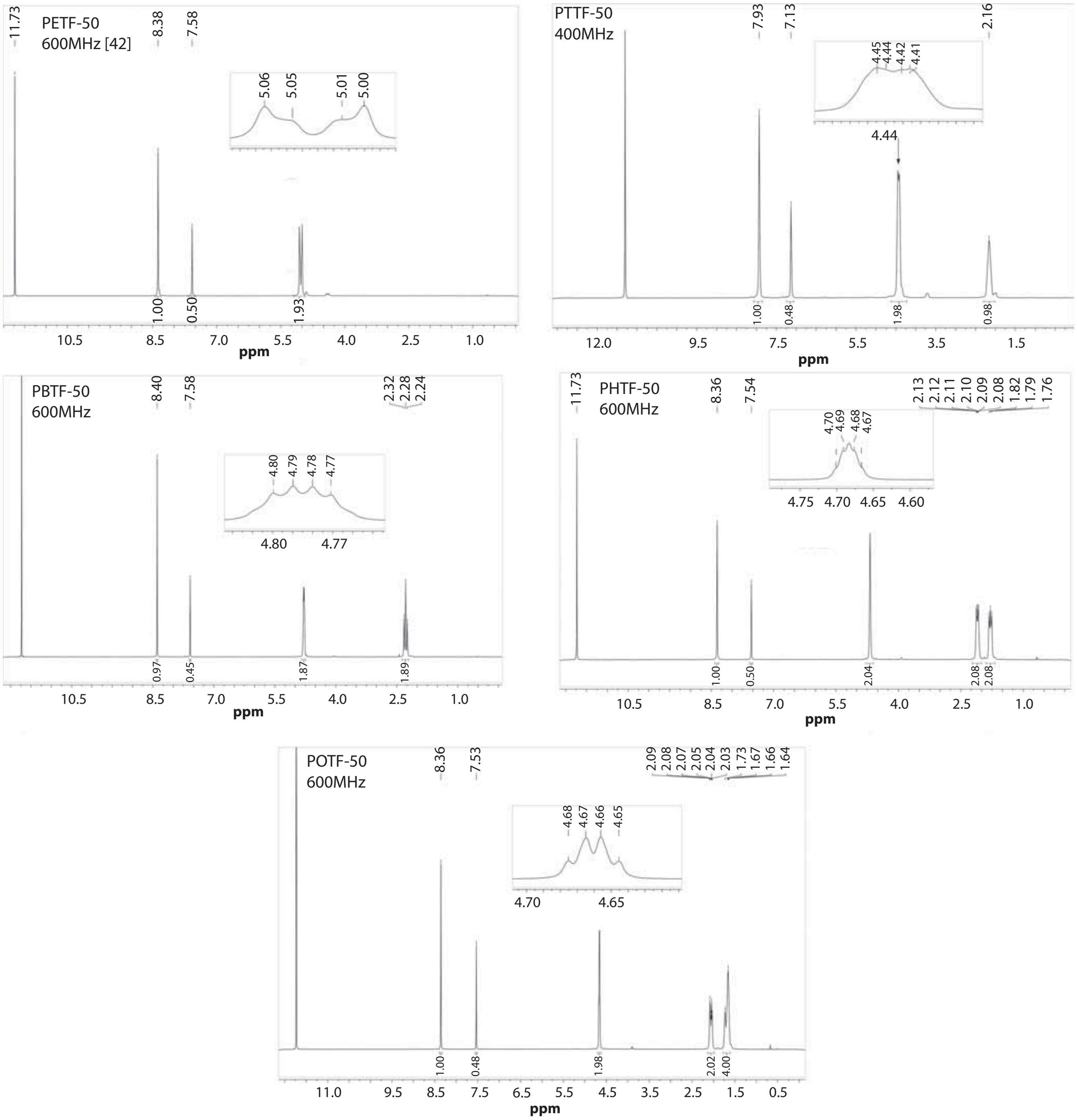

Figure 1 The ^{1}H-NMR spectra of copolyesters.

from P1–P5. As shown in Table S1, the peak area ratios of two asymmetric structures of the coployester unit were in accord with theoretical and real mole ratios of TPA and FDCA in copolyesters, which further showed that five copolyesters were random copolymers. The results in Table S1 were calculated according to the formulas of Yamadera and Murano [46].

The presence of crystallinities of copolyesters at original ecology were assessed by XRD (Figure 3). For PETF copolyester series, they were all amorphous polyesters similar to PEF and PET at original ecology. For PTTF copolyester series, PTTF-10 diffractogram showed well-defined sharp signals similar to that of PTT (2θ=15.3, 16.8, 19.4, 21.7°) [45]. On the contrary,

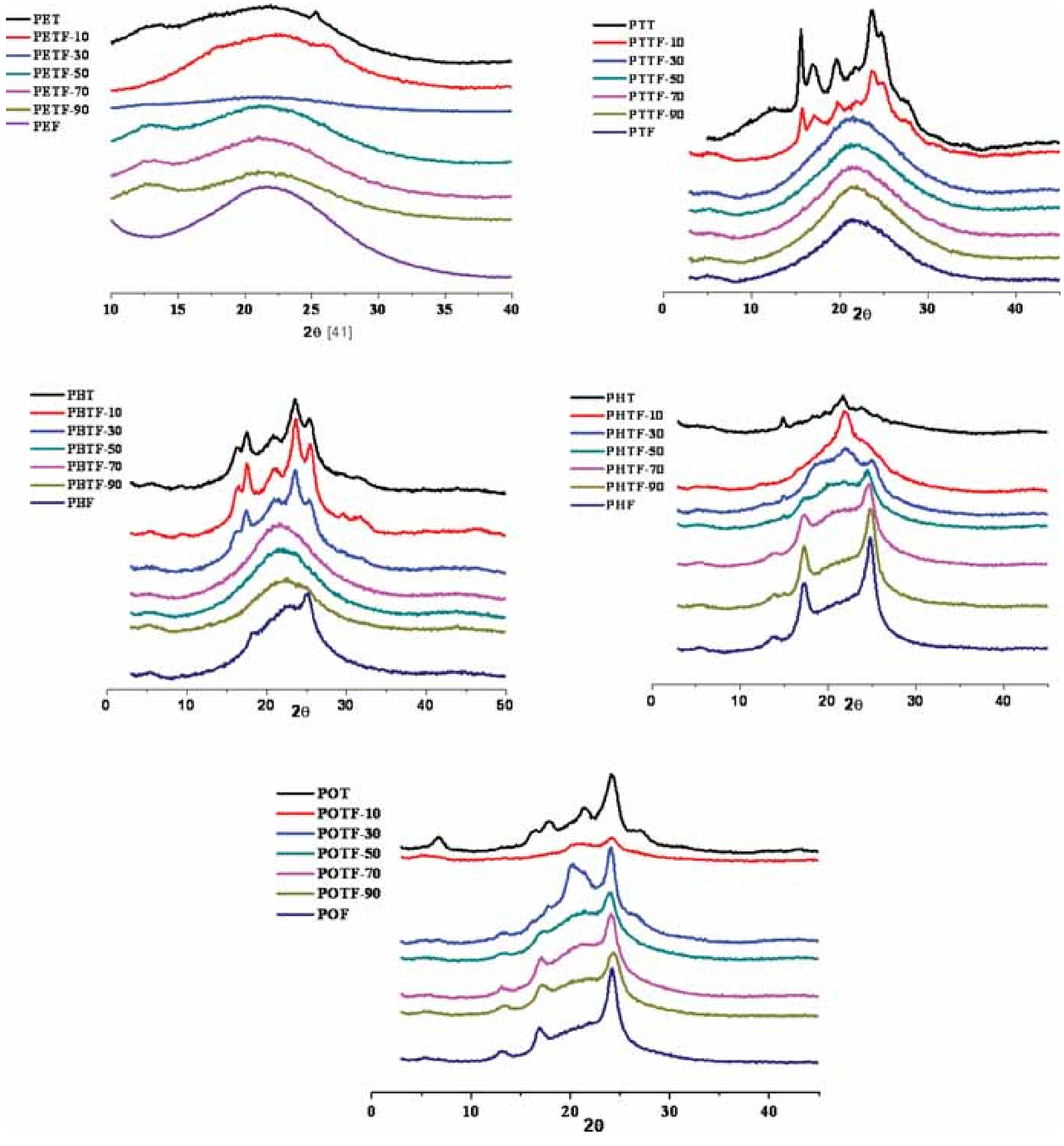

Figure 2 The XRD patterns of copolyesters.

when the number of PTF units increased, such as PTTF-30 and PTTF-50, the copolyesters appeared to be completely amorphous, similar to PTF at original ecology. For PBTF copolyester series, PBTF-10 and PBTF-30 diffractograms appeared to have similar signals compared to that of PBT (2θ=16.1, 17.2, 20.2, 23.2, 25.1) [46]. However, PBTF-50, PBTF-70 and PBTF-90 were absolutely amorphous polyester, different from that of PBT and PBF. For PHTF copolyesters, it was obvious that the signals in their diffractograms tended to be similar to those of PHF (2θ=13.00, 16.74, 24.31°) [38], with the number of PHF units increasing. For

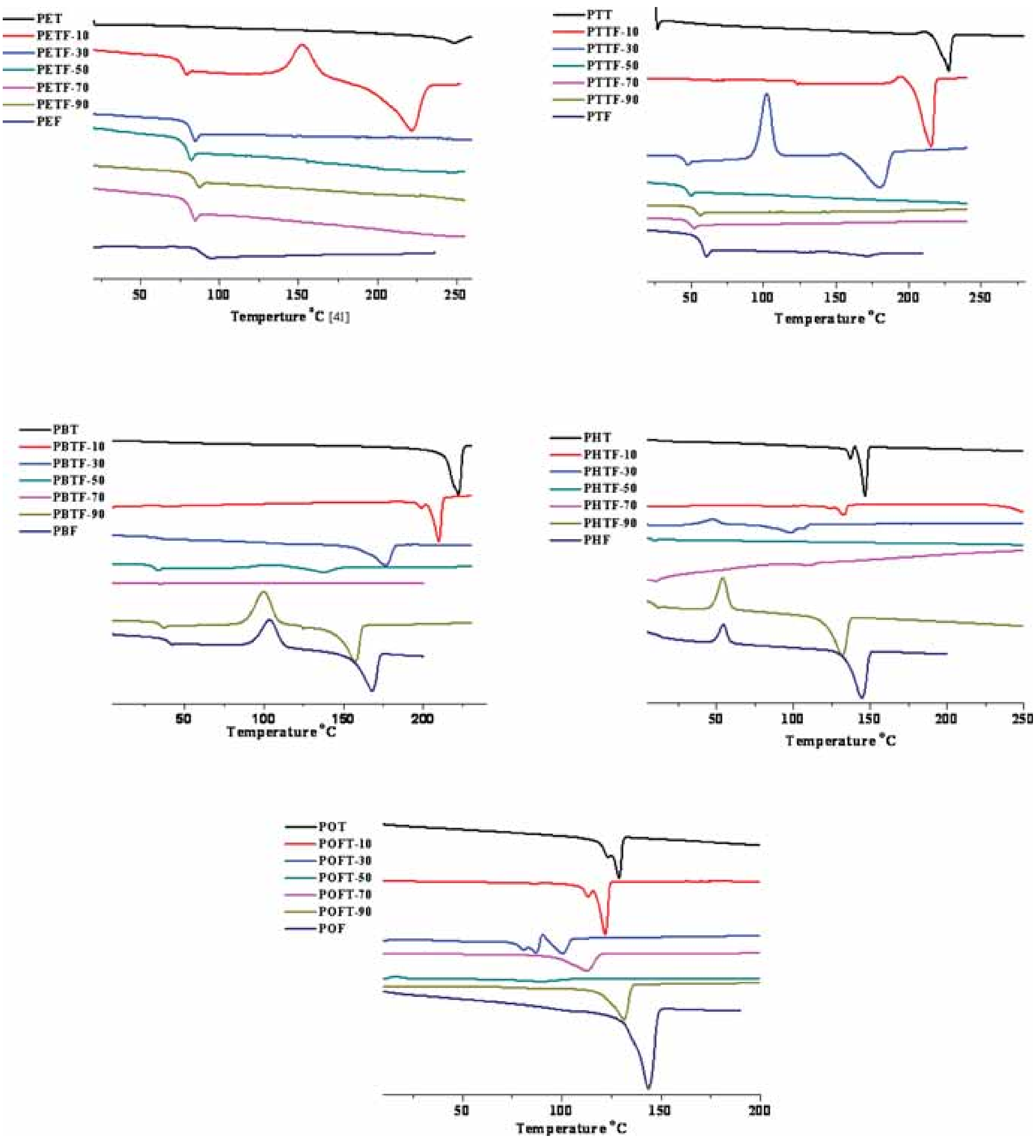

Figure 3 The DSC tracings of copolyesters.

POTF copolyester series, the trend of the signals in their diffractograms was similar to that of PHTF with increasing POF units (POF $2\theta=12.39$, 16.33, 23.48°) [38]. Although the structures of TPA and FDCA were similar, the benzene ring of TPA could rotate freely and the rotation of the furan ring on the copolyester backbone was hindered. The FDCA-based polyester unit and TPA-based polyester unit each disturbed the structure of the other in copolyesters, and therefore the crystallization did not occur, especially when the methylene number of diol was less in the copolyesters chain, such as in PETF, PTTF and PBTF copolyesters. However, the interaction of the TPA-based polyester unit and FDCA-based polyester unit was lower, with the number of methylene increasing in the copolyester chain. So when the FDCA-based polyester unit was higher, the well-defined sets of crystalline diffraction peaks of copolyesters were similar to those of

Table 4 The results of DSC and TGA of copolyesters.

	DSC		TGA				DSC		TGA		
Sample	**T_g(°C)**	**T_m(°C)**	**T_d(°C)**	**T_{dm}(°C)**	**Level of residue (LR) (%)**	**Polyester**	**T_g(°C)**	**T_m(°C)**	**T_d(°C)**	**T_{dm}(°C)**	**Level of residue (LR) (%)**
PET[41]	72.0	257.1	407.4	440.0	17.10	PHT	28.5	146.5	384.1	412.9	6.04
PETF-10[41]	73.3	218.4	407.3	431.0	19.39	PHTF-10	28.2	132.6	374.8	400.7	11.26
PETF-30[41]	76.7	no	405.9	436.7	11.25	PHTF-30	22.9	97.6	375.0	397.8	8.73
PETF-50[41]	78.7	no	393.3	413.4	17.35	PHTF-50	22.8	no	374.3	394.6	12.30
PETF-70[41]	81.1	no	392.6	417.8	14.69	PHTF-70	26.1	110.0	373.4	388.5	8.20
PETF-90[41]	84.2	no	391.7	411.9	14.27	PHTF-90	30.6	131.8	369.8	389.9	6.84
PEF[41]	85.1	210.4	370.9	405.5	13.86	PHF	33.5	144.6	370.0	387.0	6.01
PTT	44.1	223.3	383.2	405.0	7.51	POT	15.9	128.9	383.9	406.5	2.24
PTTF-10	44.6	215.3	380.8	403.28	10.04	POTF-10	13.7	121.9	380.7	398.0	6.64
PTTF-30	44.6	180.1	377.5	404.9	8.98	POTF-30	12.1	111.3	382.2	401.3	4.49
PTTF-50	45.9	no	377.2	397.0	9.83	POTF-50	13.5	111.7	375.7	405.8	5.15
PTTF-70	47.8	no	371.2	392.0	7.12	POTF-70	16.1	112.6	374.2	398.5	4.43
PTTF-90	51.9	no	370.5	390.4	13.48	POTF-90	21.3	131.2	376.6	405.3	3.96
PTF	56.1	no	370.0	393.3	8.83	POF	23.0	143.7	370.4	386.5	3.95
PBT	48.6	221.9	383.1	403.2	11.97						
PBTF-10	36.2	209.6	382.9	399.7	10.38						
PBTF -30	34.1	176.2	377.7	402.2	8.13						
PBTF -50	31.4	138.5	370.4	391.3	9.34						
PBTF-70	31.4	no	370.7	392.1	11.72						
PBTF-90	33.3	157.9	370.0	389.6	8.71						
PBF	36.9	168.8	366.4	383.8	7.02						

*T_g: the glass-transition temperature, T_m: melting point T_d: the initial thermal decomposed temperature, T_{dm}: temperature at the maximum degradation rate

FDCA-based homopolyesters, for example, the PHTF and POTF copolyester series.

The DSC thermograms (Figure 4) showed that all of the copolyesters exhibited glass transition temperatures (T_gs) ranging from 12 to 85°C, depending on the ratios of FDCA-based polyester unit to TPA-based polyester unit in the copolyester structure and the structure of diols used. The thermal history of copolyesters during the second heating run after the samples were removed is shown in the DSC thermograms in Figure 4. The T_gs of all copolyesters were between those of TPA-based homopolyesters and FDCA-based

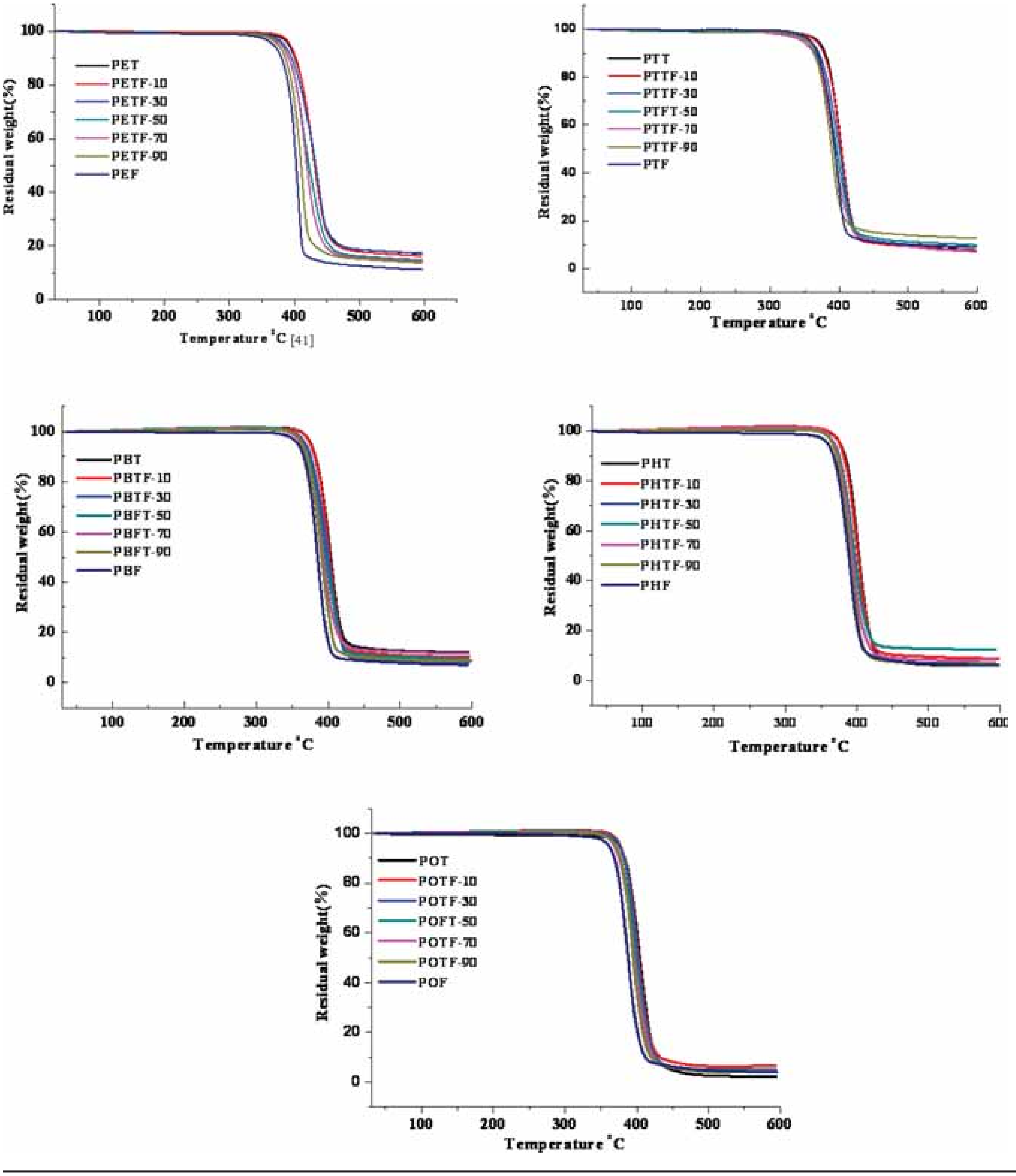

Figure 4 The TGA thermographs of copolyesters.

homopolyesters which, on the other hand, displayed the formation of random copolyesters. Furthermore, in the same copolyester series, for example, the PETF copolyester series, the T_g values increased with the increasing number of FDCA-based polyester units, which was mostly caused by the stiffness of FDCA-based polyester unit which was stronger than that of TPA-based polyester unit. As one could anticipate, the T_g of copolyester with long methylene chain was lower than that of copolyester with short methylene chain. For example, the T_g of POTF-50 was lower than that of PETF-50. In PETF copolyesters, PETF-10, which has 10% mol/mol PEF unit incorporated into the copolyester backbone, was semicrystalline, with its DSC tracing displaying a cold crystallization peak at 156.3°C and a melting peak at 218.4°C. In the PTTF copolyester series, PTTF-10 and PTTF-30 had melting peaks at 215.3 and 180.1°C, and the cold crystallization temperature (T_c) of PTTF-30 was 102.3°C. In the PBTF copolyester series, except for PBTF-70 in which the content of PBF unit was 70% (mol/mol), the other copolyesters had T_ms. In addition, PBTF-90 had T_c at 99.7°C. For the PHTF copolyester series, PHTF-10, PHTF-30, PHTF-70 and PHTF-90 had T_ms and PHTF-50 had no T_m. For the POTF copolyester series, all copolyesters had T_ms ranging from 111.3 to 131.2°C. It was clear that the insertion of FDCA-based polyester unit into the copolyesters' backbones had a strong effect on the crystallization of the copolyesters.

The TGA thermographs of copolyesters (Table 4 and Figure 5) exhibited three major characteristic features: the initial thermal decomposition temperature (T_d) of 370 to 410°C, temperature at the maximum degradation rate (T_{dm}) of 380 to 440°C and the level of residue of 3 to 20%. All of the copolyesters had one thermal decomposition step. These behaviors were similar to that displayed by TPA-based homopolyesters and FDCA-based homopolyesters, albeit with somewhat lower thermal stability than that of TPA-based homopolyesters. The T_d was mostly associated with the methylene chain of copolyesters. The T_{dm} was mostly caused by the furan unit and benzene unit of the copolyesters, because the corresponding TPA-based homopolyesters and FDCA-based homopolyesters degraded at similar temperatures. The thermal stability of copolyesters became slightly lower than that of TPA-based homopolyesters with increasing FDCA-based polyester unit, because the furan ring was the heteroatomic ring and its thermal stability was lower than that of the aromatic benzene ring. For example, the T_d and T_{dm} values of PETF-90 were lower than those of PETF-10. In the research work of Sousa *et al.*, PET-ran-PEF copolyester showed two maximum degradation temperatures of approximately 400 and 450°C, which they explained as most probably associated with the degradation of the furanic and benzenic units of copolyesters, because the corresponding PEF and PET homopolyesters degrade at different temperatures of 398 and 440°C respectively. However, in our research work, PETF copolyesters had one maximum degradation temperature and the other copolyesters also had only one. This difference from Sousa *et al.* might have been caused by the different synthesis method (direct esterification method vs ester exchange method) and different molecular weight of the copolyesters. In addition, it was clear that all of the copolyesters had the level of residue of 3 to 20%.

Table 5 listed the tensile modulus (Et), tensile strength (σm) and elongation at break (εb) data of copolyesters. From Table 5 it can be seen that the association of FDCA-based polyester units into copolyesters' backbones had a strong effect on their mechanical properties. And there was no rule to follow this effect. The Et-σm values of FDCA-based homopolyesters were somewhat larger than those of TPA-based homopolyesters. For example, the Et-σm values of PEF were a little larger than those of PET. Their εb values were similar. For the PETF copolyesters series, the Et values of PETF-10, PETF-70 and PETF-90 were larger than that of PET. The σm values of PETF-10, PETF-30, PETF-70 and PETF-90 were larger than that of PET. The εb values of PETF-50, PETF-70 and PETF-90 were similar to that of PEF and PET. It was obvious that PETF-10, PETF-70 and PETF-90 had better mechanical properties and were better than that of PET. For the PTTF copolyesters series, the Et and σm of all copolyesters were lower than that of PEF. However, PTTF-70 and PTTF-90 had better Et than that of PTT; and PTTF-30, PTTF-50 and PTTF-70 hold better σm than that of PTT. It made PTTF-10, PTTF-50 and PTTF-70 have a larger εb than that of PEF and PET via the introduction of FDCA-based polyester units into the copolyesters' backbones. In a word, PTTF-70 had better mechanical property than that of PTT. For the PBTF copolyesters series, the Et and σm values of all copolyesters were smaller than that of PBF. Only PBTF-10 had larger Et and σm than that of PBT. Surprisingly, all of the PBTF copolyesters had larger εb (>298%) than that of PBF and PBT. PBTF-10 held a similar mechanical property to PBT. For the PHTF copolyester series, their Et values were smaller than that of PHT and PHF. The σm values of PHTF-70 and PHTF-90 were larger than that for PHT and PHF. Inside, the PHTF-10 had the largest εb (917.0%). All of the PHTF copolyesters had good elongations at break. For the POTF copolyester series, their Et values were smaller than that of POF and POT. And only POTF-30, POTF-50 and POTF-90 had better σm than that of POT. Obviously, all of the POTF copolyesters had larger elongations at break. In

Table 5. Mechanical properties (Tensile modulus, Et. Tensile strength, σ_m and Elongation at break, ε_b) of PTTF, PBTF, PHTF, POTF copolyesters and PTT, PTF, PBT, PBF, PHT, PHF, POT, POF polyesters

Mechanical	E_t (MPa)	σ_m(MPa)	ε_b (%)	Sample	E_t (MPa)	σ_m (MPa)	ε_b (%)
PET[41]	1115.0	25.1	2.3	PHT	502.0	28.2	467.0
PETF-10[41]	1235.0	55.9	74	PHTF-10	221.0	28.2	563.0
PETF-30[41]	951.0	59.5	52	PHTF-30	118.0	19.4	577.0
PETF-50[41]	1004.0	21.8	2.2	PHTF-50	14.8	19.1	917.0
PETF-70[41]	1295.0	48.1	4.3	PHTF-70	62.9	36.8	705.0
PETF-90[41]	1400.0	56.9	4.5	PHTF-90	251.0	32.6	165.0
PEF	1555.0	25.6	1.5	PHF	833.0	37.4	156.7
PTT	1055.0	42.0	4.2	POT	218.0	25.8	323.0
PTTF-10	912.0	41.1	47.3	POTF-10	200.0	24.1	510.0
PTTF-30	953.0	45.3	6.6	POTF-30	109.0	27.7	793.0
PTTF-50	943.0	49.5	43.0	POTF-50	98.0	31.8	757.0
PTTF-70	1313.0	56.4	44.0	POTF-70	124.0	24.7	307.0
PTTF-90	1440.0	11.3	0.9	POTF-90	200.0	40.3	350.0
PTF	1790.0	57.3	4.3	POF	338.0	32.8	223.3
PBT	1168.0	45.5	175.0				
PBTF-10	1203.0	46.7	298.0				
PBTF-30	740.0	32.1	323.0				
PBTF-50	526.0	33.6	590.0				
PBTF-70	534.0	32.5	516.0				
PBTF-90	722.0	32.1	403.0				
PBF	1483.0	56.8	5.2				

general, POTF-10 and POTF-90 had similar mechanical properties to that of POT. The copolymerization of FDCA and TPA contributed to enhancing the tensile modulus and tensile strength of TPA-based polyesters, especially when the number of methylene was between 2 to 4 in certain mole ratios. When the number of methylene was 6 and 8, the association of FDCA-based polyester units into copolyester backbone was good enough to enhance the elongation at break.

4 CONCLUSION

Five novel copolyester series were synthesized based on FDCA, TPA and diols (ethylene glycol, 1,3-propanediol, 1,4-butanediol, 1,6-hexanediol and 1,8-octanediol) via direct esterificaiton method by using TBT as catalyst. The direct esterification method was applied with good results to prepare not only FDCA-based and TPA-based homopolyesters, but also TPA-FDCA-diol copolyesters. ^{1}H-NMR confirmed the expected structures of copolyesters. The copolyesters had different degrees of brown color compared with the white of the TPA-based homopolyesters, in which the color darkened gradually with increased FDCA content in the copolyesters. All of the copolyesters were random copolymers (B=1.0 and 1.40) and had higher molecular weight. In TPA, FDCA and diol nucleophilic substitution reaction, the reactive activity of TPA and FDCA to diol was similar, especially when TPA and FDCA reacted with long chain diol. The morphology at original ecology, T_g, T_m, T_c, T_d, T_{dm}, tensile modulus (Et), tensile strength (σm) and elongation at break (εb) of copolyesters were seriously affected by the chain structure and chain composition of the copolyesters. All of the copolyesters had one T_g. They increased with the increase of FDCA-base units in the same series and the T_gs decreased by increasing the number of methylene compared with different copolyester series. The copolyesters had similar thermal properties to that of corresponding FDCA-based homopolyesters and TPA-based homopolyesters. However, there was no rule for following the effect on morphology at original ecology, crystallinities and tensile properties when FDCA-based units were incorporated into copolyester backbone. Some of the copolyesters have good mechanical properties compared with corresponding TPA-based homopolyesters. In summary, the properties endowed copolyesters based on renewable resources make them a viable alternative to their successful petrochemical TPA-based counterpart for use as biopolymer materials in the future.

ACKNOWLEDGEMENT

The authors thank the National Nature Science Foundation of China (Project No: 51103152) for financial support.

REFERENCES

1. B.J. Nikolau, M.A.D.N. Perera, L. Brachova1, B. Shanks, Platform biochemicals for a biorenewable chemical industry. *Plant. J.* **54**, 536–545 (2008).
2. J.B. van Beilen, Y. Poirier. Production of renewable polymers from crop plants. *Plant J.* **54**, 684–701 (2008).
3. M.N. Belgacem, A. Gandini, Eds. *Monomers Polymers and Composites from Renewable Resources*, Elsevier: Amsterdam (2008).
4. S. Inkine, M. Hakkarainen, A.C. Albertsson, A. Södergård. From Lactic Acid to Poly(lactic acid) (PLA): Characterization and Analysis of PLA and Its Precursors *Biomacromolecules*. **12** (3), 523–532 (2011).
5. A. Corma, S. Iborra, A. Velty. Chemical routes for the transformation of biomass into chemicals. *Chem Rev.* **107** (6), 2411–2502 (2007).
6. L.M. Lara, W.H. Gjalt. Metabolic Engineering of Poly (3-Hydroxyalkanoates): From DNA to Plastics *Microbiol. Mol. Biol. Rev.* **63**, 21 (1999).
7. J. Zhao, W.Q. Yu, C. Chen, H. Miao, H. Ma, Q. Song. A remarkable enhancement of catalytic activity for KBH 4 treating the carbothermal reduced Ni/AC catalyst in glycerol hydrogenolysis. *Catal. Lett*. **134**, 184–189 (2010).
8. E. Taarning, I.S. Nielsen, K. Egeblad, R. Madsen, C.H. Christensen. Chemicals from renewables: Aerobic oxidation of furfural and hydroxymethylfurfural over gold catalysts. *ChemSusChem.***1** (1–2), 75–78 (2008).
9. Y. Román-Leshkov, J.N. Chheda, J.A. Dumesic. Phase modifiers promote efficient production of hydroxymethylfurfural from fructose. *Science* **312**, 1933–1937 (2006).
10. H. Zhao, J.E. Holladay, H. Brown, C. Zhang. Metal chlorides in ionic liquid solvents convert sugars to 5-hydroxymethylfurfural. *Science* **316**, 1597–1600 (2007).
11. S. Dutta, S. De, B. Saha. A Brief Summary of the Synthesis of Polyester Building-Block Chemicals and Biofuels from 5-Hydroxymethylfurfural *Chempluschem* **77** (4), 259–272 (2012).
12. A. Gandini, M.N. Belgacem. Furans in polymer chemistry. *Prog. Polym. Sci*. **22**, 1203–1397 (1997).
13. E. DeJong, R. Dam, L. Sipos, D. Den Ouden, G.J. Gruter. Furandicarboxylic Acid (FDCA),A Versatile Building Block for a Very Interesting Class of Polyesters Abstracts of Papers of the American Chemical Society. **241**, 404 (2011).
14. T. Werry, G. Peterson. *Top Value Added Chemicals from Biomass*, U.S. Department of Energy, Washington, DC. (2004).
15. C.N.D. Neumann, W.D. Bulach, M. Rehahn, R. Klein. Water-free synthesis of polyurethane foams using highly reactive diisocyanates derived from 5-hydroxymethylfurfural. *Macromol. Rapid Comm.* **32** (17), 1373–1378 (2011).
16. N. Okhay, N. Mignard, C. Jegat, M. Taha. Diels–Alder thermoresponsive networks based on high maleimide-functionalized urethane prepolymers. *Des. Monomers Polym.* **16** (5), 475–487 (2013).
17. O. Grosshardt, U. Fehrenbacher, K. Kowollik, B. Tubke, N. Dingenouts. Synthese und Charakterisierung von Polyestern und Polyamiden auf der Basis von Furan-2, 5-dicarbonsäure. *Chem IngTech*. **81** (11), 1829–1835 (2009).
18. J.F. Galan, C.N. Tang, S. Chakrabarty, Z.W. Liu, G. Moyna, V. Pophristic. Conformational preferences of furan- and thiophene-based arylamides: a combined computational and experimental study *Phys. Chem. Chem. Phys*. **15** (28), 11883–11892 (2013).
19. S. Toshiyuki, H. Kisaburo, H. Yoshikazu. Syntheses of Polyesters Containing Furan Ring *Kogyo Kagaku Zasshi*. **63**, 176–178 (1960).
20. J.A. Moore, J.E. Kelly. Polyesters derived from furan and tetrahydrofuran nuclei. *Macromolecules* **11** (3), 567–573 (1978).
21. A. Gandini, A.J. Silvester, C.P. Neto, A.F. Sousa, M. Gomes. The Furan Counterpart of Poly (ethylene terephthalate): an Alternative Material Based on Renewable Resources *J. Polym. Sci. Part A: Polym. Chem.* **47** (1), 295–298 (2009).
22. M. Gomes, A. Gandini, A.J. Silvester, B. Reies. Synthesis and Characterization of Poly(2,5-furan dicarboxylate)s Based on a Variety of Diols *J. Polym. Sci. Part A: Polym. Chem.* **49**, 3759–3768 (2011).
23. E. Gubbels, L. Jasinska-Walc, C.E. Koning. Synthesis and characterization of novel renewable polyesters based on 2, 5-furandicarboxylic acid and 2, 3-butanediol. *J. Polym. Sci. Part A: Polym. Chem.* **51**, 890–898 (2013).
24. J.P. Ma, X.F. Yu, J. Xu, Y. Pang. Synthesis and crystallinity of poly (butylene 2, 5-furandicarboxylate). *Polymer* **53**, 4145–4151 (2012).
25. J.H. Zhu, J.L. Cai, W.C. Xie, P.H. Chen, M. Gazzano, M. Scandola, R.A. Gross. Poly (butylene 2, 5-furan dicarboxylate), a biobased alternative to PBT: synthesis, physical properties, and crystal structure. *Macromolecules* **46**, 796–804 (2013).

26. T. Pan, J. Deng, Q. Xu, Y. Zuo, Q.X. Guo, Y. Fu. Catalytic Conversion of Furfural into a 2, 5-Furandicarboxylic Acid-Based Polyester with Total Carbon Utilization. *ChemSusChem*. **6**, 47–50 (2013).
27. J.P. Ma, Y. Pang, M. Wang, J. Xu, H. Mab, X. Nie. The copolymerization reactivity of diols with 2, 5-furandicarboxylic acid for furan-based copolyester materials. *J. Mater. Chem*. **22**, 3457–3461 (2012).
28. A.J.J.E. Eerhart, A.P.C. Faaij, M.K. Patel. Replacing fossil based PET with biobased PEF; process analysis, energy and GHG balance. *Energy Environ. Sci.* **5**, 6407–6422 (2012).
29. E. de Jong, M.A. Dam, L. Sipos, G.-J.M. Gruter. ACS Symposium Series; American Chemical Society: Washington, DC, 2012. Chapter 1: 1–13
30. J.G.N. Drewitt, J. Lincoln, Br. Patent 621971, (November 12, 1946).
31. L.B. Wu, R. Mincheva, Y.T. Xu, M.R. Raquez, P. Dubois. High molecular weight poly (butylene succinate-co-butylene furandicarboxylate) copolyesters: From catalyzed polycondensation reaction to thermomechanical properties. *Biomacromoleculars* **13**, 2973–2981 (2012).
32. J.P. Ma, Y. Pang, M. Wang, J. Xu, H. Ma, X. Nie. The copolymerization reactivity of diols with 2, 5-furandicarboxylic acid for furan-based copolyester materials. *J. Mater. Chem*. **22**, 3457–3461 (2012).
33. Z.L. Yu, J.D. Zhou, F. Cao, B. Wen, X. Zhu, P. Wei. *J. Appl. Polym. Sci.* **130** (2), 1415–1420 (2013).
34. A.F. Sousa, M. Matos, C.S.R. Freire, A.J.D. Silvestre, J.F. New Copolyesters Derived From Terephthalic and 2,5-Furandicarboxylic Acids: A Step Forward in The Development of Biobased Polyesters Coelho. *J. Polym.* **54**, 513–519 (2013).
35. J.J. Wang, J.W. Ren, X.H. Liu, G.Z. Lu, Y.Q. Wang. High yield production and purification of 5-hydroxymethylfurfural. *Aiche J.* **59** (7), 2558–2566 (2013).
36. J.S. Kruger, V. Choudhary, V. Nikolakis, D.G. Vlachos. Elucidating the Roles of Zeolite H-BEA in Aqueous-Phase Fructose Dehydration and HMF Rehydration. *ACS Catal.* **3** (6), 1279–1291 (2013).
37. X.M. Zhou, Z.H. Zhang, B. Liu, Z. Xu, K.J. Deng. Microwave-assisted Rapid Conversion of Carbohydrates into 5-Hydroxymethylfurfural by ScCl3 in Ionic Liquids *Carbohydr Res.* **375**, 68–72 (2013).
38. M. Jiang, Q. Liu, Q. Zhang, C. Ye, G.Y. Zhou. A series of furan-aromatic polyesters synthesized via direct esterification method based on renewable resources. *J. Polym. Sci. Part A: Polym. Chem.* **50**, 1026–1036 (2012).
39. Q. Liu, M. Jiang, G.Y. Zhou, Q. Zhang, C. Ye, Y.H. Ao. Anti-HIV activity of medicinal herbs: usage and potential development. *Chin J. Appl. Chem.* **29**, 752–756 (2012).
40. M. Jiang, Q. Liu, Y. Li, Q. Zhang, G.Y. Zhou. Synthesis and Characteration of Poly (Ethylene 2,5-Furandicarboxylate) *Acta Polymerica Sinica* (1), 24–29 (2013).
41. L.G. Li, Y. Li, Ch. Ye, Q. Zhang, M. Jiang, G.Y. Zhou. *Chin. J. Appl. Chem.* **30** (6), 661–666 (2013).
42. M. Jiang, T.T. Lu, G.W. Jiang, Q. Zhang, G.Y. Zhou. Synthesis and characteration of poly(ethylene terephthalate-co-ethylene 2, 5-furandicarboxylate). *Acta Polymerica Sinica* (8), 1092–1098 (2013).
43. T.T. Lu, M. Jiang, Q. Zhang, G.Y. Zhou, G.F. Wu. Sequence Structures of Poly(Ethylene Terephthalate-Co-Ethylene 2,5-Furandicarboxylate) via 1H-NMR and 13C-NMR *Chin. J. Analyt. Chem.* **42** (8), 1117–1123 (2014).
44. J. Scheirs, T.E. Long, Eds. *Modern Polyesters: Chemistry and Technology of Polyesters and Copolyesters*. John Wiley & Sons, West Sussex, U.K., 2003.
45. Z. Jedilinski, D. Sek, B. Dziewiecka. *Eur. Polym. J*, **13**, 871–874 (1977).
46. J.R. Wei. *Thermoplastic Polyester and its Application*. Chemical Industry Press, Bei Jing. 2011.
47. Z.H. Gan, K. Kazuhiro, Y. Motonori, A. Hideki, D. *Yoshiharu*. *Polym Degrad Stabil.* **83** (2), 289–300 (2004).

Supplemental Data

Gauss peak separation method was used to separate peak.
Cut-paper weighting method was selected to calculate peak area.

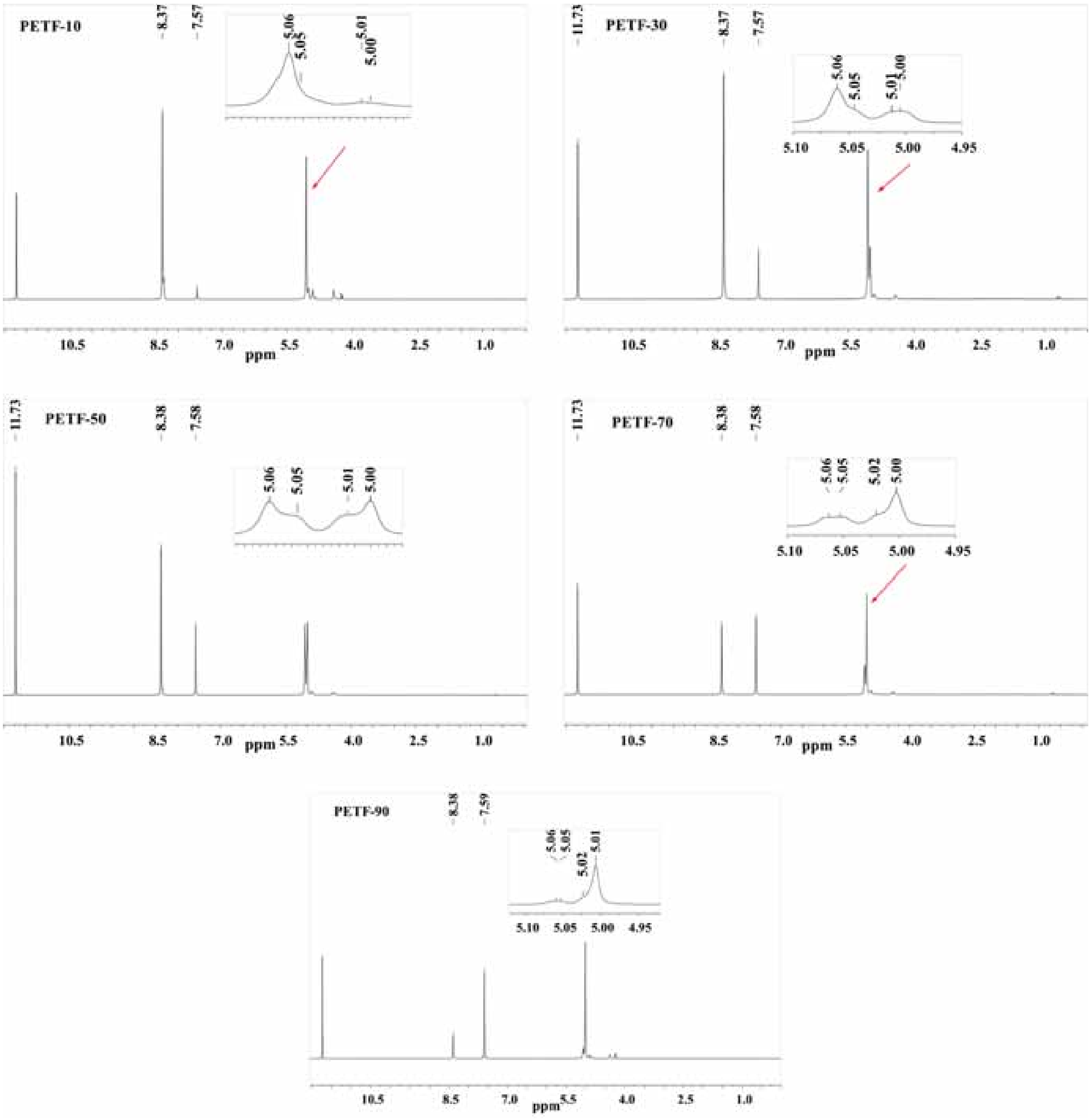

P1 ^{1}H-NMR spectra of PETF copolymers (600MHz).

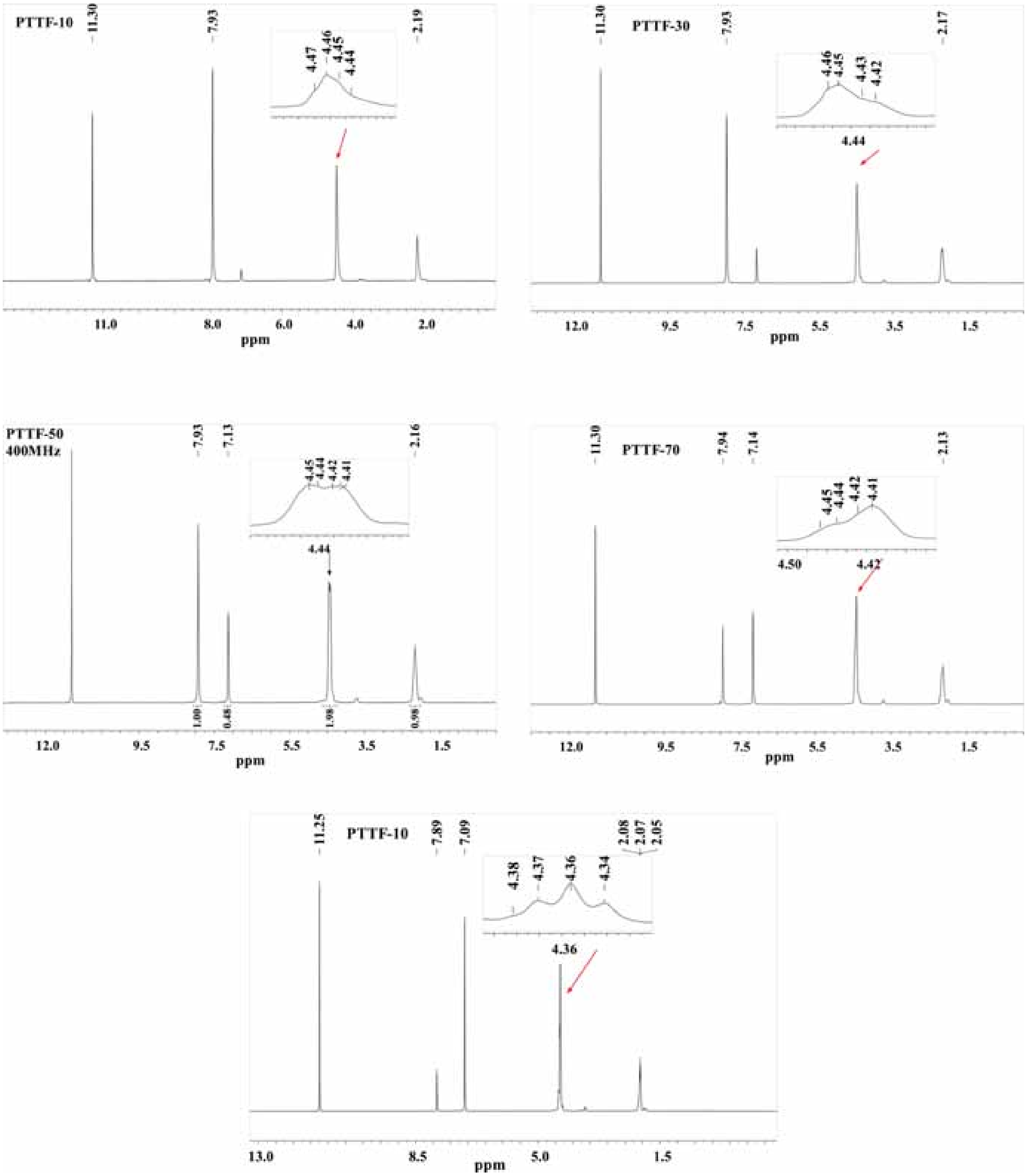

P2 ^{1}H-NMR spectra of PTTF copolymers (400MHz).

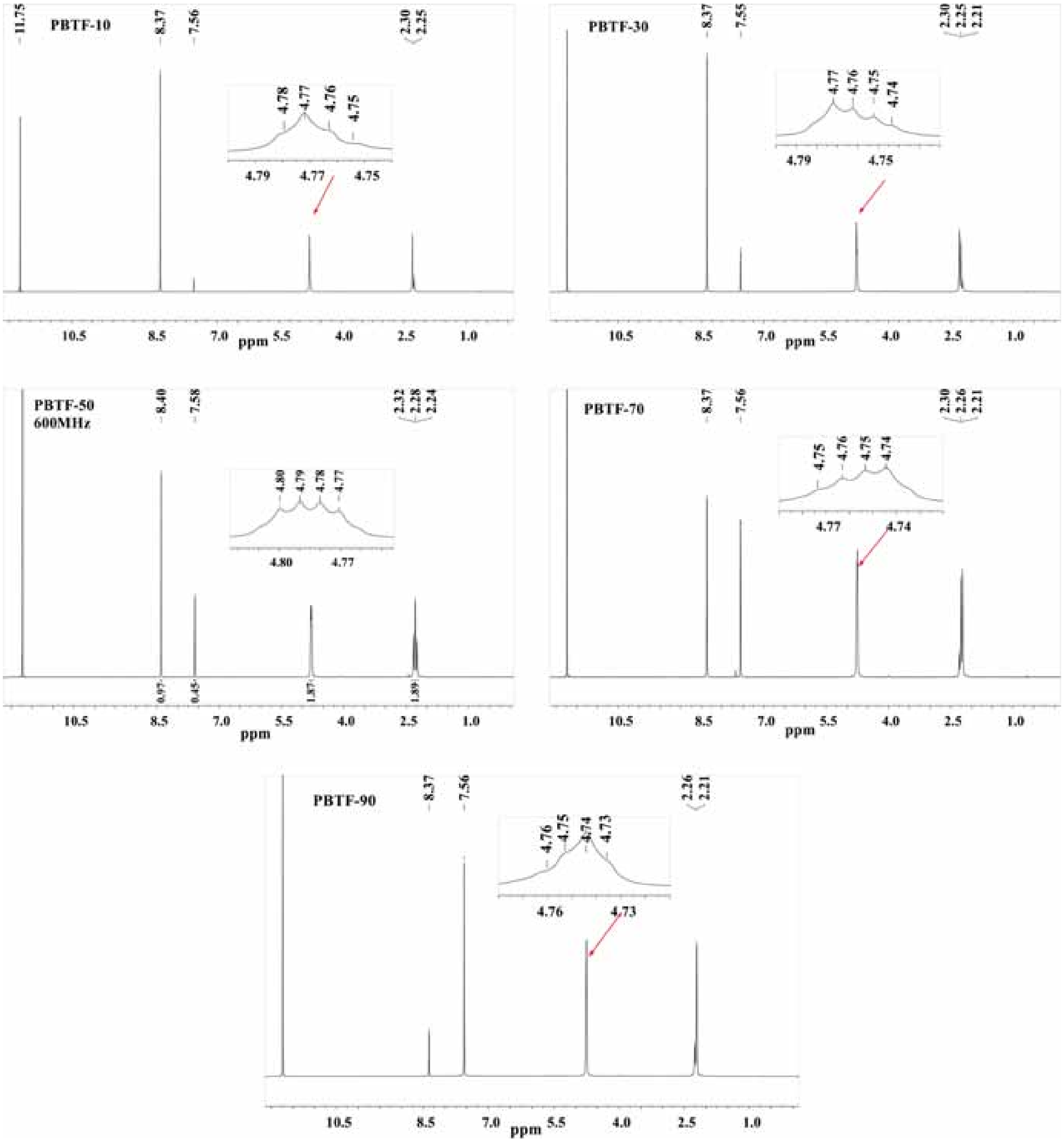

P3 ^{1}H-NMR spectra of PBTF copolymers (600MHz).

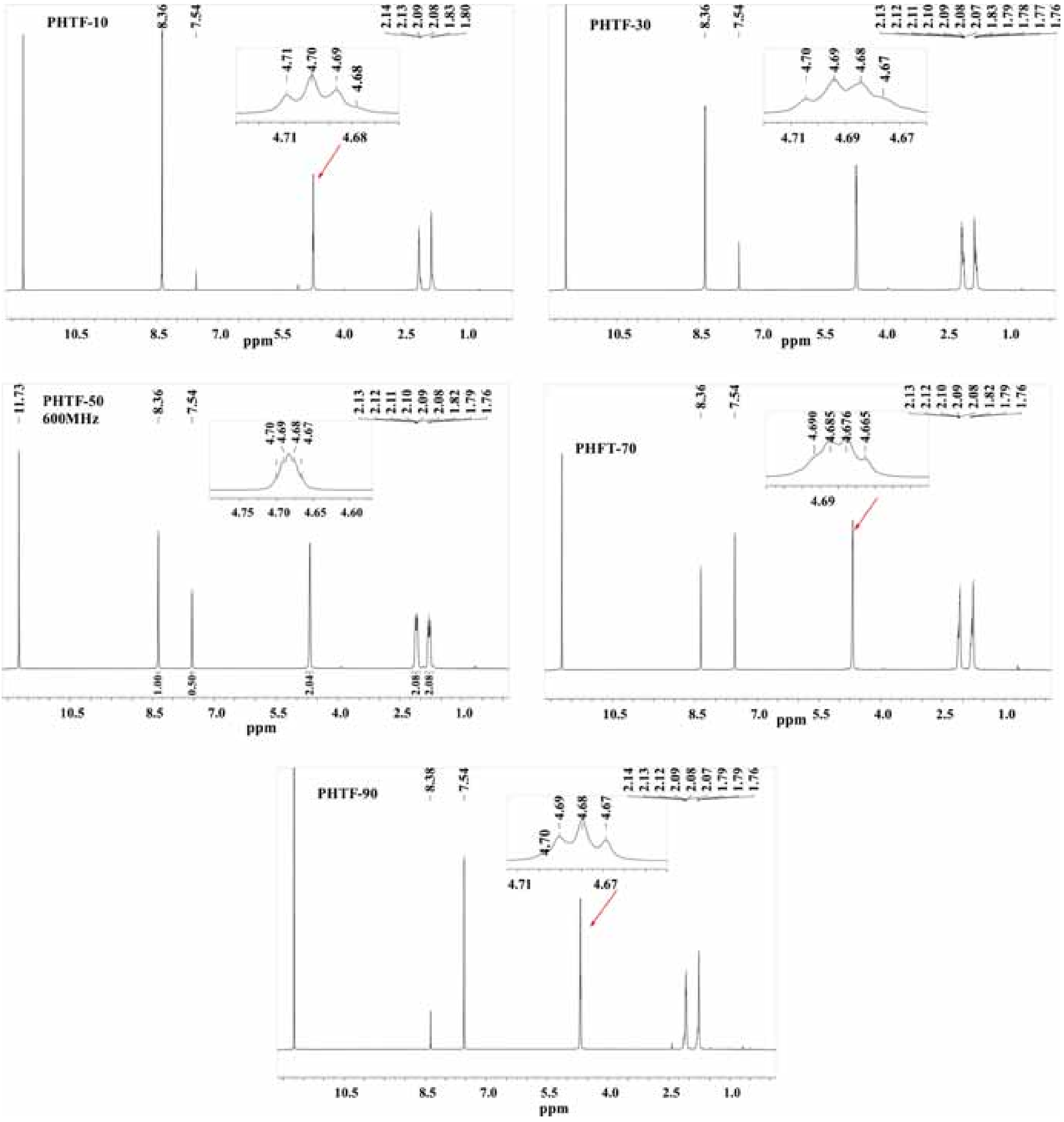

P4 ^{1}H-NMR spectra of PHTF copolymers (600MHz).

For terpolymer (A-C-B), P_A and P_B can be calculated from intensity of the corresponding peak in NMR spectra. P_A and P_B are the mole fraction of unit ACA and unit BCB from the formulas of Yamadera and Murano [46]. P_{ACA}, P_{BCB} and P_{ACB} are triad peak area for unit ACA, unit BCB and unit ACB.

$$P_A=1/2P_{ACB}+P_{ACA} \quad (1)$$

$$P_B=1/2P_{ACB}+P_{BCB} \quad (2)$$

Probability of unit AC proceeds to unit BC:

$$P_{AB}=P_{ACB}/2P_A \quad (3)$$

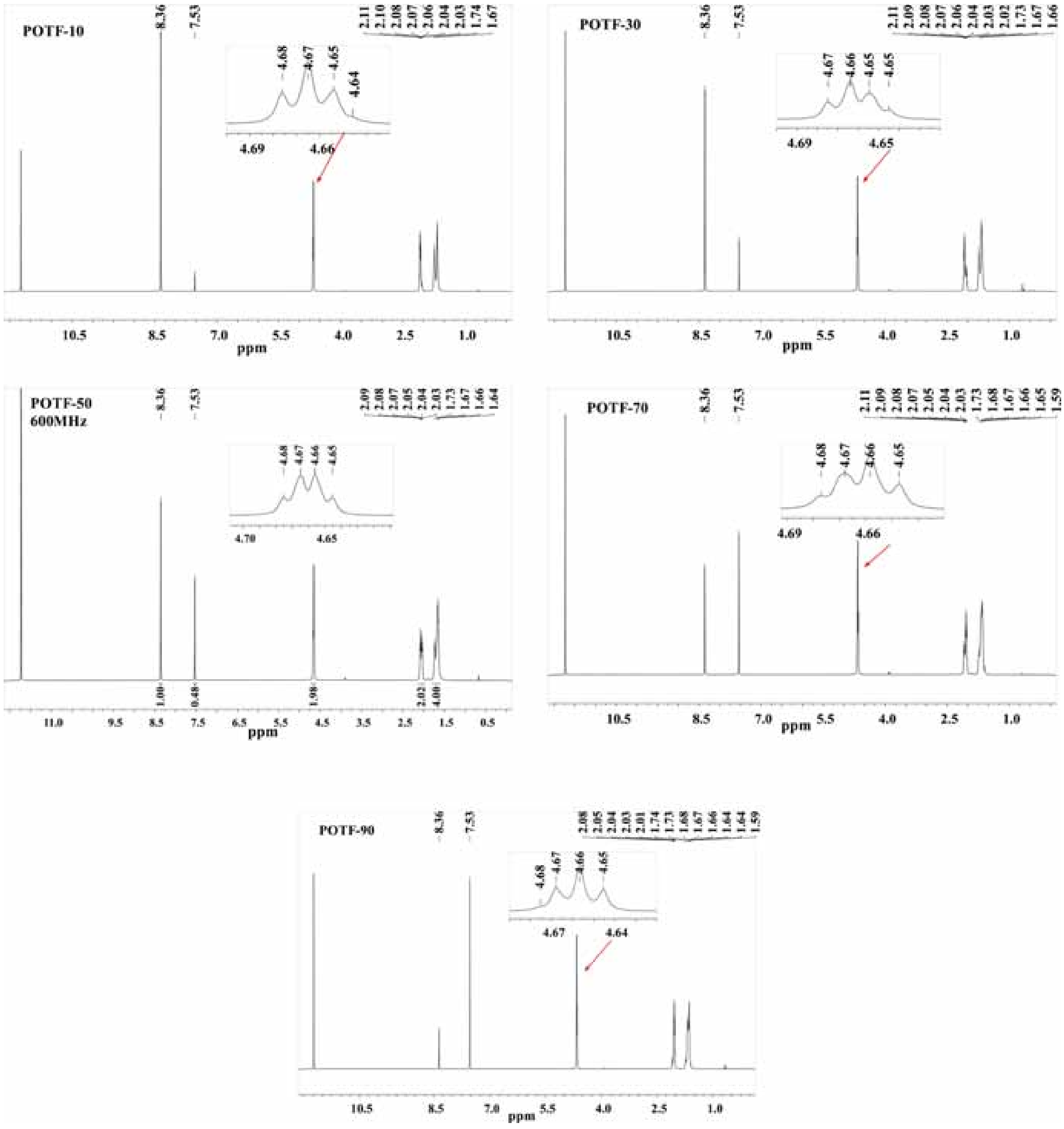

P5 ^{1}H-NMR spectra of POTF copolymers (600MHz).

Probability of unit BC proceeds to unit AC:

$$P_{BA}=P_{ACB}/2P_B \quad (4)$$

The degree of randomness (B):

$$B=P_{AB}+P_{BA} \quad (5)$$

Mean sequence length:

$$L_{AC}=1/P_{AB} \quad (6)$$

$$L_{BC}=1/P_{BA} \quad (7)$$

Table S1 lists the calculated results from the formulas of Yamadera and Murano [46].

Table S1. The influence of the mole ratios of PTA and FDCA in the initial reaction mixture on the structure of polymer chains in different copolyesters by ^{1}H-NMR.

Copolyesters	Content of structure (%)				Unit content, mole fractions randomness		Probability of finding of units		Block length		Degree of randomness
	P_{ACA}	P_{ACB}	P_{BCB}	P_{ACA}:P_{BCB}	P_A	P_B	P_{AB}	P_{BA}	L_{AC}	L_{BC}	B
PETF-10	54.7	39.5	5.8	0.94:0.10	0.745	0.255	0.265	0.775	3.774	1.290	1.040
PETF-30	34.4	50.0	15.6	0.66:0.30	0.59	0.406	0.421	0.616	2.375	1.623	1.036
PETF-50	24.0	51.4	24.6	0.49:0.50	0.497	0.503	0.517	0.511	1.934	1.957	1.028
PETF-70	17.1	46.4	36.5	0.33:0.70	0.403	0.597	0.576	0.389	1.736	2.571	0.965
PETF-90	7.7	34.9	57.4	0.12:0.90	0.251	0.749	0.695	0.233	1.439	4.292	0.928
PTTF-10	49.4	45.0	5.6	0.88:0.10	0.719	0.281	0.313	0.801	3.195	1.248	1.11
PTTF-30	31.4	55.4	13.2	0.71:0.30	0.591	0.409	0.469	0.677	2.132	1.477	1.15
PTTF-50	25.2	49.6	25.2	0.50:0.50	0.500	0.500	0.496	0.496	2.020	2.020	0.99
PTTF-70	15.1	49.2	35.7	0.30:0.70	0.397	0.603	0.620	0.408	1.613	2.451	1.03
PTTF-90	4.9	49.6	45.5	0.10:0.90	0.297	0.703	0.835	0.353	1.200	2.833	1.19
PBTF-10	53.3	40.6	6.1	0.87:0.10	0.736	0.264	0.276	0.769	3.623	1.300	1.04
PBTF-30	35.7	49	15.3	0.70:0.30	0.602	0.398	0.407	0.616	2.457	1.623	1.02
PBTF-50	25.4	49.8	24.6	0.52:0.50	0.503	0.495	0.495	0.503	2.020	1.988	1.00
PBTF-70	16	48.6	35.4	0.32:0.70	0.403	0.597	0.603	0.407	1.658	2.457	1.01
PBTF-90	5.7	41.6	52.7	0.10:0.90	0.265	0.735	0.785	0.283	1.274	3.534	1.07
PHTF-10	32.2	64.2	3.6	0.89:0.10	0.643	0.357	0.499	0.899	2.004	1.112	1.40
PHTF-30	19.2	72.6	8.2	0.70:0.30	0.555	0.445	0.654	0.816	1.529	1.225	1.47
PHTF-50	16	68	16	0.50:0.50	0.500	0.500	0.680	0.680	1.471	1.471	1.36
PHTF-70	8.4	72	19.6	0.30:0.70	0.444	0.556	0.811	0.647	1.233	1.546	1.46
PHTF-90	3.4	65.2	31.4	0.10:0.90	0.360	0.640	0.906	0.509	1.104	1.965	1.42
POTF-10	33	63.4	3.6	0.92:0.10	0.647	0.353	0.490	0.898	2.041	1.114	1.39
POTF-30	21.3	69.6	9.1	0.70:0.30	0.561	0.439	0.620	0.793	1.613	1.261	1.41
POTF-50	15.8	68.4	15.8	0.50:0.50	0.500	0.500	0.684	0.684	1.462	1.462	1.37
POTF-70	10.2	67.6	22.2	0.32:0.70	0.440	0.560	0.768	0.604	1.302	1.656	1.365
POTF-90	3.7	65	31.3	0.11:0.90	0.362	0.638	0.898	0.509	1.114	1.965	1.41